Arabian Journal of Chemistry (2022) **15**, 103950

King Saud University

Arabian Journal of Chemistry

www.ksu.edu.sa
www.sciencedirect.com

ORIGINAL ARTICLE

Phytochemical profiling, molecular docking, and *in vitro* anti-hepatocellular carcinoid bioactivity of *Suaeda vermiculata* extracts

Hamdoon A. Mohammed [a,b,*], Suliman A. Almahmoud [a], Minhajul Arfeen [a], Ashish Srivastava [c], Mahmoud Z. El-Readi [d,e], Ehab A. Ragab [b], Safia M. Shehata [f], Salman A.A. Mohammed [g], Ehab M. Mostafa [b,h], Hend A. El-khawaga [i], Riaz A. Khan [a,*]

[a] *Department of Medicinal Chemistry and Pharmacognosy, College of Pharmacy, Qassim University, Qassim 51452, Saudi Arabia*
[b] *Department of Pharmacognosy and Medicinal Plants, Faculty of Pharmacy (Boys), Al-Azhar University, Cairo 11884, Egypt*
[c] *Department of Pharmacy, Pranveer Singh Institute of Technology (PSIT), Kanpur, UP 209305, India*
[d] *Department of Clinical Biochemistry, Faculty of Medicine, Umm Al-Qura University, Makkah 21955, Saudi Arabia*
[e] *Department of Biochemistry, Faculty of Pharmacy, Al-Azhar University, Assiut 71524, Egypt*
[f] *Clinical Pathology Department, Ain Shams University Hospitals, Cairo, Egypt*
[g] *Department of Pharmacology and Toxicology, College of Pharmacy, Qassim University, Qassim 51452, Saudi Arabia*
[h] *Department of Pharmacognosy, College of Pharmacy, Jouf University, Sakaka, Aljouf 72341, Saudi Arabia*
[i] *Botany and Microbiology Department, Faculty of Science, Al-Azhar University (Girls Branch), Cairo, Egypt*

Received 15 February 2022; accepted 4 May 2022
Available online 11 May 2022

KEYWORDS

Suaeda vermiculata;
Anti-cancer;
Liver cancer;
Hepatocellular carcinoma;
Molecular modeling;
Receptor docking;
HepG2;
HepG-2/ADR;
In vitro activity;

Abstract The ATP-binding cassette is the major class of transporters responsible for the efflux of chemotherapeutic agents from cancer cells, resulting in treatment failures of cancer's patients. *Suaeda vermiculata* Forssk. ex. J. F. Gmel. is traditionally known for its liver protective activity. The LC-MS based chemical profilings of the sequentially partitioned sub-extracts obtained from the alcoholic extract of *S. vermiculata* using *n*-hexane, chloroform, ethyl acetate, and *n*-butanol as fractionating solvents, identified a total of thirty six compounds. These sub-extracts were evaluated for their anti-hepatocarcinoma activity against the sensitive HepG2 and doxorubicin (DOX)-resistant, HepG-2/ADR cell lines. A mixture of doxorubicin and sub-extracts at 20 µg/ml doses were also tested for their anti-hepatocarcinoma activity. The exhibited IC_{50} values for the

* Corresponding authors at: Department of Medicinal Chemistry and Pharmacognosy, College of Pharmacy, Qassim University, Qassim 51452, Saudi Arabia (H.A. Mohammed, R.A.Khan).
E-mail addresses: ham.mohammed@qu.edu.sa (H.A. Mohammed), ri.khan@qu.edu.sa (Riaz A. Khan).
Peer review under responsibility of King Saud University.

Production and hosting by Elsevier

https://doi.org/10.1016/j.arabjc.2022.103950

MTT assays

chloroform, ethyl acetate, *n*-hexane, and *n*-butanol sub-extracts, and the doxorubicin against HepG2, and HepG-2/ADR cell lines were found at 64.5, 66.8, 81.25, 125, 1.3 µg/ml, and 110.1, 91.82, 138.2, 265.7, 4.77 µg/ml levels, respectively. However, the treatment of resistant cells with 20 µg/ml of different sub-extracts in combination with the doxorubicin showed significant improvements in the doxorubicin activity against the resistant cells, and the IC_{50} values for DOX + chloroform, DOX + ethyl acetate, DOX + *n*-hexane, and DOX + *n*-butanol against resistant cells, were at 1.77, 2.05, 2.66, and 2.71 µg/ml levels, respectively. The IC_{50} values exhibited 2.69x, 2.33x, 1.79x and 1.76x-folds reversal of the sensitivity in the resistant cancer cell lines. The molecular docking studies of the compounds identified in the LC-MS chemical profilings, against three ATP-binding cassette proteins *i.e.*, ABCB1, ABCC1, and ABCG2, showed that flavonoids as the major class of compounds responsible for reversal of the resistant cells sensitivities. The predicted binding affinity for the flavonoids against the above mentioned three ATP-binding cassette proteins' are in the ranges of ~−8 to −11 kcal/mol. Our results clearly indicate that the presence of flavonoids, as the major class of compounds in the *S. vermiculata* is responsible for the chemosensitization of the resistant HCC-cell lines. Moreover, the structures, **21** (5-O-methyl visamminol), **22** (N-*trans*-feruloyl tyramine), **27** (atractylenolide-III), and **32** (ginsenoside-Rh2) were also identified among the potential ATP-binding cassette's modulators during the current study. These observations put the *S. vermiculata* in perspective with the traditionally claimed liver protective efficacy of the plant.

1. Introduction

Hepatocellular carcinoma (HCC) is one of the leading causes of peoples' sufferings, and deaths across all countries of the world. It is responsible for over 70 to 90 % cases of primary liver cancers, and approximately 500,000 peoples are diagnosed every year with HCC (Shen et al., 2021). Chemotherapy, is considered one of the effective methods for the treatment of HCC, however, due to the resistatnce, the use of chemotherapeutic agents has become challenging (Le Grazie et al., 2017). Multidrug resistance (MDR) is cause of concern, and it is the main reason for treatment failures in 90 % of the cases, which is also supplemented by the recurrences (Longley and Johnston, 2005). The documented reports indicated three major mechanisms for drug resistance; (i) decreased absorption of drugs into the cancer cells, (ii) mutation in the genetic composition of the cancer cells causing the loss of cytotoxic effects of drugs, and (iii) ATP dependent efflux of the drugs from the cancer cells (Szakács et al., 2006). The ATP (Adenosine triphosphate), or energy dependent efflux of the chemotherapeutic agents is among one of the major, and well-established mechanism of drug resistance, and it is because overexpression of the involved transporter proteins. One of the major class of proteins actively involved in MDR is ATP-binding cassette, or ABC transporters (El-Awady et al., 2017). The P-glycoprotein (Pgp/ABCB1), multidrug resistance protein 1 (MRP1/ABCC1), and breast cancer resistance protein (BCRP/ABCG2), are the major types of ABC-transporters involved in the efflux of the anti-cancers drugs across the cells membranes (Bugde et al., 2017; Orlando and Liao, 2020). The ABC transporters have demonstrated significant scope for wide variety of substrates. For example, dasatinib and imatinib, the promising anti-cancer agents, are translocated out of the cancer cells by P-gp, and BCRP, causing reduction in the efficacy of the drugs, and failure of the treatment (Dohse et al., 2010). Therefore, altering the activity of transporters, or chemosensitization is considered one of the effective strategies to counteract resistant cancer cells, in addition to the identification of new chemotherapeutic agents (Szakács et al., 2006). However, until now, no small molecule has been approved by United States FDA for clinical use.

In this context, the plants-based products, as part of alternative and complementary medicine, have offered feasible replacement(s), and adjuvant to modern anti-cancer chemotherapies. The use of medicinal plants, the plants' derived preparations, extracts, fractions, concoctions, and isolated compounds, in treatment of liver disorders, including liver cancer types, have been a long tradition (Li and Martin, 2011). Accordingly, several compounds obtained from the plants sources have been reported, which can resensitize the resistance cancer cells, and reinstate the efficacy of the available chemotherapeutic agents. For example Frión-Herreraa *et al.* demonstrated chemosensitization of doxorubicin (DOX) resistant human colon cancer cells using Cuban propolis, and nemorosone (Frión-Herrera et al., 2019). Li and Lee *et al.* showed chemosensitization of tanshinone-IIA, an active ingredient isolated from *Salvia miltiorrhiza*, against DOX resistant breast cancer cells, and HCC (Lee et al., 2010; Li and Lai, 2017). Similarly, Li *et al.* showed chemosensitizing effects of quercetin in DOX-resistant human breast cancer cells (Chen et al., 2018; Li et al., 2018). Also, Choi *et al.* showed decursin, isolated from *Angelica gigas,* as a chemosensitizing agent for DOX-resistant ovarian cancer cells (Choi et al., 2016). Borska *et al.* displayed P-gp modulating capacity of quercetin against DOX-resistant human pancreatic carcinoma (Borska et al., 2010). Kim *et al.* demonstrated chemosensitizing effects of resveratrol on resistant breast cancer cells (Kim et al., 2014). In addition, fingolimod, a derivative of myriocin, and a metabolite from a traditional Chinese medicine, *Isaria sinclairii,* was shown to possess chemosenstizing effects on the DOX and etoposide-resistant colon cancer cells through the alteration of P-gp and MRP1 (Xing et al., 2014). A recent report also showed resensitizing effects of sophoraflavanone, isolated from *Sophora flavescens*, on lung

cancer cells (Wu et al., 2021). Besides, the quercetin was extensively studied for its chemosensitizing effects against various types of resistant cancer cells, and have been documented as the modulator of various transporters (Chen et al., 2010). In addition, an efficient review is available on the roles of natural products as MDR modulators (Kumar and Jaitak, 2019). The structures of some of the ABC modulators identified from the natural sources are listed in Fig. 1 as referral examples.

The *S. vermiculata,* an edible halophyte from the family Amaranthaceae, is traditionally well-known for its hepatoprotective activity. Several biological activities, e.g., antimicrobial, antioxidant, anti-inflammatory, hepatoprotective, and antidepressant activities, have been reported for the plant extracts and/or its essential oils (Al-Omar et al., 2021; Al-Tohamy et al., 2018; Mohammed, 2020; Mohammed et al., 2019a, 2020; Wang et al., 2022). The current report is an important extension of our previous work in reference to the hepatoprotection and cytotoxic efficacy of the *S. vermiculata* extract (Mohammed et al., 2019b; Mohammed et al., 2020b), dwells upon the investigation of the extract, fractions, and chemically-profiled compounds' roles in the HCC resistant cell lines. It also investigates the roles of phytochemical constituents in HCC chemosensitization through molecular modeling studies. The present study demonstrates, (i) the chemosensitizing, and anticancer effects of *S. vermiculata* fractions (*n*-hexane, chloroform, ethyl acetate, and *n*-butanol), (ii) LC-MS chemo-profilings of these fractions, (iii) molecular docking observations using Autodock vina® against binding sites of ATP-binding cassette (ABC) transporter (ABCB1, MRP1, ABCC1 and ABCG2) proteins to deduce the efficacy and severity of the anti-cancer activities of the fractions, and the compounds role in an *in silico* set-up.

2. Materials and methods

2.1. Plant materials, and extraction procedure

The aerial parts of the plant were collected in September 2019 from the arid areas of Buraydah city, Qassim Province, Saudi Arabia. The plant was identified as *S. vermiculata* Forssk by Prof. Ahmed El-Oglah, Department of Biological Sciences, Yarmouk University, Irbid, Jordan. The voucher specimen was saved at the Department of Medicinal Chemistry and Pharmacognosy, College of Pharmacy, Qassim University (voucher # 78). The plant aerial parts were dried in complete shade for three weeks, and grinded to a coarse powder before the extractions. 300 g of the dried plant material was extracted three successive times using 95 % water–ethanol mixture (3 × 1 L, aqueous ethanol). The combined aqueous ethanolic extract was dried under reduced pressure, and below 40 °C. The dried aqueous ethanolic extract was then suspended in 500 ml of distilled water, and sequentially fractionated between *n*-hexane, chloroform, ethyl acetate, and *n*-butanol (300 ml each) solvents. These four fractions were dried under reduced pressure, below 45 °C using a rotatory evaporator, and stored at –20 °C in a freezer till further work.

2.1.1. Liquid chromatography-mass spectrometry (LC-MS) analysis

Bruker Daltonics (Bremen, Germany) Impact II ESI-Q-TOF system equipped with Bruker Daltonics Elute UPLC system (Bremen, Germany) was used for fractions scanning. Specific standards were used to identify the analyte's *m/z* exact retention times after chromatographic separations. Accurately, 1 mg of the fractionated extract was dissolved in 2.0 ml of DMSO (analytical grade), centrifuged at 4000 rpm for 2.0 min, and 1.0 ml of the clear solution was transferred to the autosampler, and the injection volume was adjusted to 3.0 µl. The instrument was operated using Ion Source Apollo II Ion Funnel Electrospray source. The instrument parameters were adjusted as: capillary voltage (2500 V), nebulizer gas (2.0 bar), nitrogen flow (8 L/min), and the dry temperature (200 °C). The mass accuracy was < 1 ppm, the mass resolution was 50,000 FSR (Full Sensitivity Resolution), and the TOF repetition rate was up to 20 kHz. The chromatographic separation was performed on C18 reverse-phase (RP) column, 100 × 2.1 mm, 1.8 µm (120 A°) from Bruker Daltonics (Bremen, Germany) at 30 °C, autosampler temperature 8.0 °C, with a total run time of 35 min using the gradient elution. The eluents were consisted of methanol/ 5 mM ammonium formate/ 0.1 % formic acid, and water/ methanol (90:10 %)/ 5 mM ammonium formate/ 0.1 % formic acid (Mohammed et al., 2021).

2.2. Cytotoxicity assay

2.2.1. Cell-lines

Human cell lines of HCC, HepG-2 were cultivated in complete media under standard conditions in 5 % CO_2, 37 °C, and free from mycoplasma. The DOX resistant hepatic cell lines, HepG-2/ADR, were developed by treating, and maintaining the cells in media supplemented with 5 µg/ml DOX. The DOX resistance was confirmed through P-gp expression as compared to the parent-sensitive cell lines using RT-PCR. The DOX-free media were applied 7–10 days before conducting any experiments.

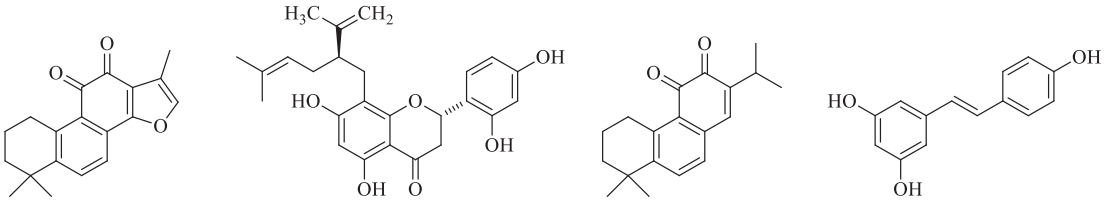

Fig. 1 Structure of some ABC modulators isolated from natural sources.

2.2.2. Cytotoxicity and reversal assays

The exponentially growing cells (2×10^3 cells/well) were seeded in 96-wells plates in MTT cell viability assays. The cells were grown for 24 hr, treated with serial concentrations of *S. vermiculata* extracted fractions (up to 1000 µg/ml), and DOX (100 µg/ml) for 24 hr, and with MTT solution (0.5 mg/ml) for 4 hr. The reaction product (crystals) were dissolved in DMSO. The absorbances were determined at 570 nm using SpectraMax M5e Multi-Mode Microplate Reader (Molecular Devices, LLC, California, USA). The same protocol was used to evaluate the cytotoxicity of the combination of DOX with *S. vermiculata* extract and fractions (20 µg/ml).

The relative resistance (RR) for the tested samples were calculated by using the following equation (Wang et al., 2021):

$$RR = \frac{\text{IC50 value obtained for the resistant cell line}}{\text{IC50 value obtained for the sensitive parental cell line}}$$

Combination index (CI): The nature of the interaction (synergy, additivity, or antagonism) between extracts and DOX were determined by the combination index (CI), as following:

$$CI = \frac{C_{DOX,50}}{IC_{50,\,DOX}} + \frac{C_{extract,50}}{IC_{50,extract}}$$

Where, $C_{DOX,50}$ is the IC_{50} value for the cytotoxic agent in a two-drug combination, and $C_{extract}$ is the fixed concentration of an extract. The $IC_{50,\,DOX,}$ and $IC_{50\ extract}$ corresponds to the IC_{50} for DOX, and extract alone. $CI < 1$ indicates synergism, $CI = 1$ indicates additive, and $CI > 1$ indicates antagonism. The synergism was confirmed by the isobologram method, and the medium effect equation.

2.3. Protein preparation and molecular dockings

Molecular dockings were performed using AutoDock Vina® v1.1.2 (Trott and Olson, 2010). The preparation of proteins, and ligands for the AutoDock Vina® involved preparing PDBQT files. The input PDB files of the proteins were prepared, and optimized by using AutoDock Tool (ADT), bundled with the MGLTools package (version 1.5.6) (Morris et al., 2009). The proteins with PDB code 6FN1, 5UJA, and 6FFC, representing ABCB1, ABCC1, and ABCG2 were downloaded from the Research Collaboratory for Structural Bioinformatics (RCSB), protein data bank (available online: https://www.rcsb.org/structure/) (Alam et al., 2019). For the proteins preparation, the co-crystallized ligands, and water molecules were deleted. The proteins molecules were corrected for missing residues and close contacts, followed by addition of polar hydrogen atoms, charges, and converted to PDBQT files using ADT. The structures of *S. vermiculata* compounds were retrieved from the PubChem database (Kim et al., 2019) as a single file in 3D-spatial data file (SDF) format. All the ligands structures were imported in Open Babel (O'Boyle et al., 2011) interface of PyRx, and were energy minimized using universal force fields, and saved as PDB files. The Gasteiger charge, and polar hydrogens were added, and ligands were set up for rotatable bonds, followed by generation of PDBQT files for the ligands (Dallakyan and Olson, 2015). The grids were generated with the autogrid4® program distributed with AutoDock®, v1.5.6. (Kalinowsky et al., 2018). The active binding sites of the proteins were chosen as the grid centers. The center grid box dimensions were chosen to include all atoms of the ligand set (Kalinowsky et al., 2018). The site of the grid box for the above mentioned three proteins have been listed in the supplementary file. The configuration text file was created (config.txt) to run AutoDock Vina® v1.1.2. This configuration file involved the receptors and ligand PDBQT file, and the coordinates for the center grid box were utilized (O'Boyle et al., 2011) (*Supplementary Data S1*). The dockings scores resulted in generation of log files. The output docking scores were defined as affinity binding (Kcal/mol), and various protein–ligand interactions, such as hydrogen bonds, and other hydrophobic interactions were analyzed using PyMol. The molecular dockings studies were performed in reference with the previous study reported by Shawky *et. al.* (Shawky et al., 2021).

2.4. Statistical analyses

All experiments were carried out in triplicates. All data are expressed as mean ± standard deviation. The IC_{50} values were calculated, and the results were presented using GraphPad Prism® software (Version 6, graph- Pad software Inc., San Diego, CA, USA). Student *t*-test was applied to determine the degree of significant differences between the sets of data, and the *p*-values < 0.05 were considered significant.

3. Results

3.1. LC-MS analyses of the S. vermiculata fractionated extracts

In an earlier report by us, a total of nine compounds were identified in the LC-MS analysis of aqueous ethanolic extract of the aerial parts of *S. vermiculata* (Mohammed et al., 2020a). The alcoholic extract was partitioned using sequential partitioning process starting with the non-polar solvent, *n*-hexane, followed by chloroform, ethyl acetate, and the polar, *n*-butanol. The gradient extraction procedure partitioned the plant's chemical constituents according to their polarity, and the solvent interaction capabilities that reflected their solubility, and partition coefficient of the corresponding constituents, provided the fractionations. However, the experimentation revealed that compounds were represented in differently-partitioned fractionated extracts in varying proportions (Table 1). In the current report, a total of 36 compounds were identified using the LC-MS based chemical profiling. The retention times of the identified compounds varied from ~ 2 to 30 min (min), and the *m*/*z* (mass) ratio varied from ~ 163 to 739 mass units. The Data Analysis 4.0 Bruker Daltonics software was used to obtain the accurate mass data and molecular formulas of the detected peaks. The comparisons with the standard authentic samples of various available compounds, the mass fragmentation patterns, and the reported phytoconstituents of genus *Suaeda* were referenced in the identification of the compounds as reported in Table 1. Additionally, the relative percentages of the identified compounds, in different fractionated extracts of the plant, were also calculated based on the total peaks area, and individual compound's peak area in the chromatograms. Twenty-four standard compounds, *i.e.*, hyperoside, isorhoifolin, chrysin, vitexin, naringenin, kaempferol, luteolin, myricetin, hesperidin, apigenin, quercetin, rhamnetin, luteolin-7-O-glucoside, chlorogenic acid, syringic acid, gallic acid, resveratrol, rosmarinic acid, 4-hydroxybenzoic acid, coumaric acid, caffeic acid, cinnamic

acid, ellagic acid, and ferulic acid, have been used in the authentication of the *S. vermiculata* constituents. Based on the used authentic samples, six flavonoids, and two phenolic acids were identified (assigned by stars (*) in Table 1). The mass fragments obtained for the glycosidic flavonoids were also used in compounds' identifications (Fig. 2). For instance, a loss of 162 atomic mass unit (amu) were observed in the mass fragmentations of hyperoside (3-*O*-galactoside of quercetin, from *m*/*z* 463.0861 $[M-H]^-$ to *m*/*z* 301.0329 $[M-H-gal]^-$) which indicated the subtraction of 162 amu of glucoside moiety. In addition, subtractions of 162 amu were also observed in the fragment spectra of kaempferol-3-*O*-glucoside (from *m*/*z* 447.0918 $[M-H]^-$ to *m*/*z* 284.0277 $[M-H-glu]^-$), apigenin-7-*O*-glucoside (mass fragment spectra showed a molecular ion peak at *m*/*z* 431.0918 $[M-H]^-$ and the aglycone peak at *m*/*z* 269.0405 $[M-H]^-$ after the fragmentation of the glucosyl moiety), spiraeoside (from *m*/*z* 463.0886 $[M-H]^-$ to *m*/*z* 301.0295 $[M-H-glu]^-$), luteolin-4′-*O*-glucoside, and luteolin-7-*O*-glucoside (from 447.0978 $[M-H]^-$ to 285.0381 $[M-H-glu]^-$, different retention times), quercetin 3-*O*-glucoside-7-rhamnoside (from 609.1427 $[M-H]^-$ to 446.0816 $[M-2H-glu]^-$). Near similar patterns of fragmentations were observed for the mass spectrum of kaempferol-3-*O*-rutinoside (*m*/*z* 593.1488 $[M-H]^-$), which demonstrated the removal of glucosyl moiety (fragment peak *m*/*z* 430.0841 $[M-H-glu]^-$) followed by the removal of rhamnosyl moiety to give the mass peak of the kaempferol aglycone. The subtraction of 308 amu was assigned for the removal of neohesperi-

Table 1 *S. vermiculata* fractionated extracts' LC-MS analysis.

Sr.	RT (min)	Mass (*m*/*z*)	MW	Ions	Identification	Presence in fractions			
						n-BuOH	EtOAc	Chloroform	*n*-Hexane
1.	2.21	165.0533	166.0606	[M−H]-	3-Phenyl lactic acid		0.0108		
2.	2.27	163.0377	164.0450	[M−H]-	Coumaric acid*	0.0681	0.1298		
3.	2.95	353.0859	354.0931	[M−H]-	Chlorogenic acid*		0.0033	0.0018	
4.	2.97	375.1296	376.1369	[M−H]-	Vitamin B2	1.4037	0.0032		
5.	2.97	167.0716	168.0789	[M−H]-	Homovanillyl alcohol	0.2008	0.00108		
6..	4.76	471.1875	472.1947	[M−H]-	Eugenol rutinoside		0.0001	0.0048	
7.	4.78	183.0274	184.0347	[M−H]-	Methylgallate			0.0004	
8.	4.89	463.0886	464.0959	[M−H]-	Spiraeoside*		0.0007		
9.	5.12	433.1099	434.1171	[M−H]-	3,4′,7-Trihydroxy isoflavanone 3-O-glucoside	0.0557			
10.	5.28	739.2096	740.2169	[M−H]-	Kaempferol 3-neohesperidoside-7-rhamnoside		0.0041	0.0009	
11.	5.54	593.1488	594.1560	[M−H]-	Kaempferol-3-O-rutinoside	0.0043	0.0002		
12.	5.6	609.1427	610.1500	[M−H]-	Quercetin 3-glucoside-7-rhamnoside	0.0043	0.1799	0.1737	0.6789
13.	5.73	463.0861	464.093	[M−H]-	Hyperoside*	0.0004	0.0084	0.0040	
14.	5.92	447.0906	448.0978	[M−H]-	Luteolin 7-O-glucoside (Cynaroside)*	0.0039	0.0107	0.0005	
15.	6.32	577.1539	578.1625	[M−H]-, [M + Cl]-	Isorhoifolin*	0.0033	0.0009		
16.	6.36	593.1472	594.1545	[M−H]-	Kaempferol 3-neohesperidoside	0.0094	0.6724	0.2166	4.4362
17.	6.57	447.0918	448.0991	[M−H]-	Kaempferol-3-O-glucoside	0.0032	0.0341	0.0051	0.0035
18.	6.81	447.0935	448.1008	[M−H]-	Luteolin-4′-O-glucoside	0.0053	0.0051		
19.	6.82	431.0962	432.1035	[M−H]-	Vitexin*	0.0090	0.0049		
20.	6.9	431.0985	432.1058	[M−H]-	Isovitexin	0.0087	0.0203		
21.	7.77	289.1097	290.1169	[M−H]-	5-O-Methyl visamminol			0.04089	0.3616
22.	8.06	312.1217	313.1290	[M−H]-	N-*trans*-Feruloyltyramine		0.0840	1.2902	0.0026
23.	8.59	301.0335	302.0407	[M−H]-	Quercetin*			0.0047	
24.	9	431.0985	432.1058	[M−H]-	Apigenin-7-O-glucoside	0.0023	0.0007	0.0008	
25.	10.35	315.0508	316.0580	[M−H]-	Rhamnetin*		0.0006	0.0043	
26.	11.7	329.2309	330.2382	[M−H]-	5,8,12-Trihydroxy-9-octadecenoic acid	0.6831	0.7213	0.8067	0.0350
27.	14.24	247.1339	248.141	[M−H]-	Atractylenolide-III	0.0108	0.0004	0.0060	
28.	14.25	293.1737	294.1810	[M−H]-	6-Gingerol	0.3559	0.2474	0.3505	0.2634
29.	20.49	293.2101	294.2174	[M−H]-	Hydroxy- octadecatrienoic acid	0.0745	0.1847	0.0343	0.0140
30.	25.68	253.2149	254.2222	[M−H]-	Hexadecenoic acid	0.1235	0.1558	0.2632	0.0953
31.	26.16	279.2304	280.2377	[M−H]-	Linoleic acid	0.3503	1.4442	1.4396	0.0721
32.	27.42	621.4395	622.4468	[M−H]-	Ginsenoside-Rh2	1.6509		0.1285	1.7994
33.	27.91	255.2308	256.2381	[M−H]-	Palmitic acid	2.8006	2.9178	2.7987	1.1694
34.	28.23	281.2464	282.2536	[M−H]-	Elaidic acid	1.8698	1.7717	2.7175	1.2159
35.	29.96	283.2620	284.2693	[M−H]-	Octadecanoic acid	9.5513	8.4236	8.4351	6.1598
36.	30.01	353.3441	354.3514	[M−H]-	n-Tricosanoic acid	0.1136	0.0340	0.0768	0.1991
Number of the tentatively identified compounds						26	31	26	15
Percentages of the identified compounds in relation to the total peaks area in the chromatogram						19.37	17.08	18.81	16.51

* Compounds identified based on authentic samples.

dose, which clearly appeared in the mass fragments of the kaempferol-3-neohesperidoside (from m/z 593.1472 $[M-H]^-$ to m/z 285.0376 $[M-H-glu-rha]^-$). The 3,4′,7-trihydroxy isoflavanone-3-*O*-glucoside mass fragmentation pattern showed the base peak of the compound at m/z 433.1099 $[M-H]^-$, followed by the aglycone peak, after removal of the glucosyl moiety, showing mass fragment at m/z 272 $[M-glu]^-$, and 275 $[M-glu + 3H]^-$. The flavonoid aglycones structures were assigned according to the mass fragmentation patterns (Fig. 2). For instance, quercetin aglycone (m/z 301.0335 $[M-H]^-$ has been compared to its authentic sample mass, and was identified based on its mass fragments m/z 178.9942, and m/z 151.0002, the two main fragments reported for the compound (Buchner et al., 2006)). Also, the rhamnetin aglycone showed the base peak at m/z 315.0452 $[M-H]^-$, and fragment ion peak at m/z 300.0225 $[M-CH_3-H]^-$, besides its identification by the comparison with the standard rhamnetin sample. The aglycone parts, kaempferol, and the luteolin, in the identified glycosides were assigned according to the small mass fragments represented in their mass spectra. For example, the presence of fragments at m/z 268, 227, 185, 107 (Fig. 2G) mass units have been reported at higher intensity in the mass spectra of kaempferol (March and Miao, 2004), while the reported mass fragments of luteolin (Li et al., 2016) represented in the glycosides containing luteolin, as a aglycone part of their structure, i.e., luteolin-4′-*O*-glucoside, and luteolin-7-*O*-glucoside, observed fragment ion peaks at m/z 151 and 133, which have been detected in these compounds containing the luteolin as the aglycone sub-structures.

The highest proportions of the compound present in these fractionated extracts was octadecanoic acid (stearic acid indicated by m/z 283.2620). The total proportions of the compound in different fractions was found to be at ~ 32%, calculated from the total peaks areas in the chromatograms (Table 1). The compounds, palmitic acid, elaidic acid, and kaempferol-3-neohesperidoside were also found to be present in significant proportions. The combined percentage of the mentioned compounds were at ~ 9 %, ~7 %, and ~ 5 %, and are shown in Table 1, with m/z ratios of 255.2308, 281.2464, and 594.1545, respectively. In addition, other compounds present in the significant ratios were ginsenoside-Rh2, linoleic acid, and 5,8,12-trihydroxy-9-octadecenoic acid. The combined ratio (in %) of these materials were found to vary between ~ 2 to ~ 3%. The compounds, 6-gingerol, *n-trans*-feruloyltyramine, and quercetin-3-glucoside-7-rhamno side were also present in notable proportions. The combined percentage quantity of these materials were present in ~ 1%. In addition, certain compounds of considerable pharmacological activity were also noted to be present in the fractions. Presence of vitexin (0.013%), isovitexin (0.029%), and cyanroside (0.015%), 3,4′,7-trihydroxy-3-O- isoflavone glucoside (0.055%), coumaric acid (0.198%), homovanillyl alcohol

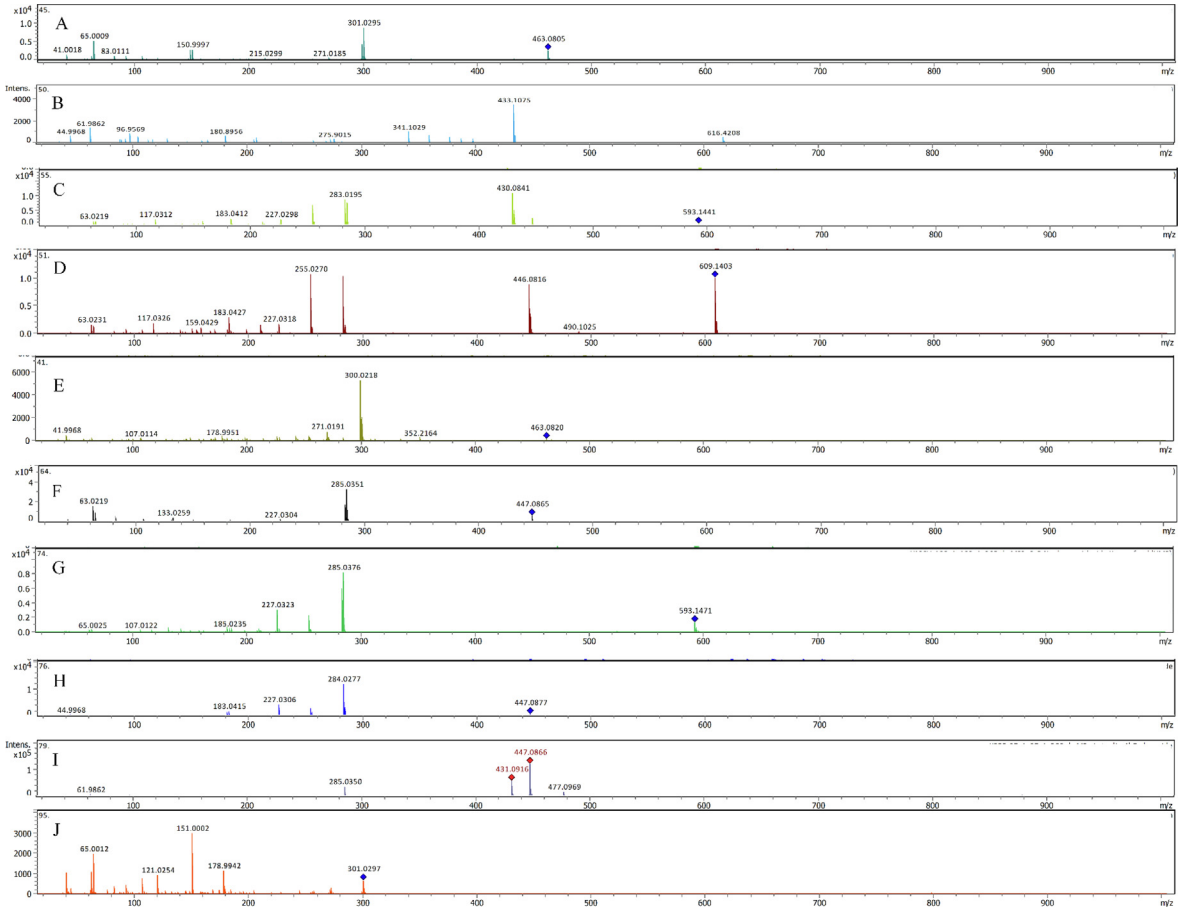

Fig. 2 (A-L): Fragmentation pattern of (A) Spiraeoside, (B) 3,4',7-trihydroxyisoflavanone-3-O-glucoside, (C) Kaempferol-3-O-rutinoside, (D) Quercetin-3-glucoside-7-rhamnoside, (E) Hyperoside, (F) Luteolin 7-O-glucoside, (G) Kaempferol-3-neohesperidoside, (H) Kaempferol-3-O-glucoside, (I) Luteolin-4'-O-glucoside, (J) Quercetin, (K) Apigenin-7-O-glucoside, (L) Rhamnetin standards.

(0.201%), kaempferol-3-*O*-glucoside (0.046%), and 5-*O*-methyl visamminol (0.402%). Also, the four fractions of *S. vermiculata* contained 26, 31, 25, and 15 numbers of constituents, representing 19.39 %, 17.08 %, 18.81 %, and 16.51 % of the total identified compounds as deduced from the total and individual peak areas in the LC-chromatograms of the *n*-butanol, ethyl acetate, chloroform, and *n*-hexane fractionated extracts, respectively. Among the total number of identified compounds, sixteen were identified as flavonoids, in which fourteen flavonoids were present in glycosylated form. The identified flavonoids were most abundant in the ethyl acetate, followed by *n*-butanol, and chloroform fractions. However, the least number of the identified flavonoids were found in the *n*-hexane fraction of the plant. The number of flavonoids present in ethyl acetate, *n*-butanol, chloroform, and *n*-hexane fractions were found to be 14, 12, 9, and 3 in numbers, respectively. The sequential distributions of the flavonoids populations are consistent with the solvent's polarities (and non-polar) extraction capacity, which was supplemented by the levels of the hydrophilic nature of the identified flavonoids (Table 1). For instance, the medium polarity of most of the identified flavonoids made them more liable to solubilize in the medium polar solvent, ethyl acetate. Moreover, the concentrations based sequential distributions of the flavonoids between the solvents was interesting and stark in nature, as it was observed that, the highest concentration of the flavonoids were localized in most non-polar solvent, *n*-hexane (5.12 % compared to the total peaks in the *n*-hexane fraction's chromatogram), as compared to 0.94 %, 0.11 %, and 0.41 % of the flavonoids compounds present in the ethyl acetate, *n*-butanol, and chloroform fraction's extract, respectively, which copuld be attributed to presence of moisture in the commercial grade *n*-hexane utilized for the purpose. A number of phenolic products were also tentatively identified in the plant extract. A total of seven phenolics were identified in the *S. vermiculata* extracted fractions, wherein 3 compounds (0.64 %) were identified in the *n*-butanol fraction, 6 compounds (0.47 %) were identified in the ethyl acetate, 5 compounds (1.65 %) were identified in the chloroform, and 2 compounds (0.27 %) were found in the *n*-hexane fractions. These results showed that among all the LC-MS chromatograms-based identified flavonoids, and phenolics constituents, four compounds were solely present in the chloroform and ethyl acetate fractions, i.e., chlorogenic acid, eugenol rutinoside, kaempferol-3-neohesperi doside-7-rhamnoside, and rhamnetin. In addition, the methyl gallate, and quercetin were only present in the chloroform fraction, while spiraeoside was present merely in the ethyl acetate fraction of the *S. vermiculata*. Nonetheless, nine fatty acids were identified in *S. vermiculata* which were distributed in all the fractionated extracts at different concentrations, *i.e.*, *n*-butanol (17.22 %), ethyl acetate (15.65 %), chloroform (16.70 %), and the *n*-hexane fractions (10.76 %).

3.2. S. vermiculata extract/fractions reverses doxorubicin (DOX) cytotoxicity in resistant hepatic cell lines

The cytotoxicity of *S. vermiculata* extract and fractions in the sensitive HepG-2 cells were conducted in comparison to the standard cytotoxic drug, DOX. Fig. 3 demonstrated the dose–response curves for the *S. vermiculata* fractions, in comparison to the standard chemotherapeutical agent DOX. The IC_{50} values for DOX in the sensitive as well as resistant HCC cell lines were found to be 1.3 and 4.77 μg/ml. Among different fractions of th extract, the most potent cytotoxic effects for sensitive HepG-2 cell lines was obsrved in the chloroform, and ethyl acetate fractions of the plant. The IC_{50} values for the corresponding fractions were 64.45, 66.68 μg/ml, respectively. For the *n*-hexane, and *n*-butanol fractions, which showed moderate inhibitory effects on the sensitive HepG-2 cancer cell lines, the IC_{50} values were found to be 81.51 and 125.00 μg/ml. The fractions were also tested against resistant HepG-2/ADR cell lines. As observed for the sensitive cell lines, the most potent activity against the resistant cell lines were observed for chloroform and ethyl acetate fractions. The IC_{50} values for the two sequentially partitioned extracts were found to be 110.1 and 91.82 μg/ml, respectively. For *n*-hexane, and *n*-butanol fractions of the extract, the IC_{50} values were noted to be 138 and 265 μg/ml, respectively. The calculated relative resistances for the four fractions of the *S. vermiculata,* i.e., chloroform, ethyl acetate, *n*-hexane, and *n*-butanol, were 1.71, 1.38, 1.70, and 2.13, respectively. The calculated relative resistance for the standard chemotherapeutic drug DOX was at 3.67 (Table 2).

The four fractionated extracts were also examined against resistant HepG-2/ADR cell lines in combination with the DOX. The resistant cells were treated with DOX in the presence, and in the absence of 20 μg/ml of the four sequentially partitioned fractions of the alcoholic extract. As evident from dose response curves, as shown in Fig. 4, the chloroform, ethyl acetate, *n*-hexane, and *n*-butanol fractions enhanced the cytotoxic effects of DOX against the resistant cancer cell lines, HepG-2/ADR. The IC_{50} values of DOX in combination with the four fractions in the DOX resistant cells are shown in Table 3. The IC_{50} values of DOX in combination with 20 μg/ml of chloroform, ethyl acetate, *n*-hexane, and *n*-butanol fractions against the resistant cancer cell lines were found to be 1.77, 2.05, 2.66, and 2.71 μg/ml, respectively. These IC_{50} values indicated 2.69x, 2.33x, 1.79x, and 1.76x folds, ($p < 0.001$), reversal of DOX cytotoxicity in the resistant cancer cell lines. The strongest cytotoxicity reversal effects of these combinations were observed for the chloroform fraction of the plant, as indicated by the combination index (CI) of 0.55. Similarly, the CI for ethyl acetate fraction was 0.56. However, the *n*-hexane, and *n*-butanol CI values were found to be at 0.70 and 0.64, respectively (Fig. 4**,** Table 3).

3.3. Molecular docking of identified compounds against ABC transporter proteins

The overexpression of ABC transporter family efflux pump is one of the main causes of DOX resistance in HCC (Cox and Weinman, 2016). Three ABC subfamilies, ABCB1 (the MDR protein), ABCC1 (MRP protein), and ABCG2 (BCRP protein) play significant roles in DOX resistance in HCC (Ng et al., 2000; Nies et al., 2001; Silverman and Thorgeirsson, 1995). In about 80 to 90 % of the HCC cases, the upregulation of P-gp, or ABCB1 protein induces DOX resistance (Cox and Weinman, 2016; Ng et al., 2000), while in 10 % of the cases, other two proteins are responsible. To evaluate our hypothesis that compounds identified in different fractions of the *S. vermiculata* alcoholic extract possess the potential to sensitize DOX-resistant HCC, and to understand the molecular level

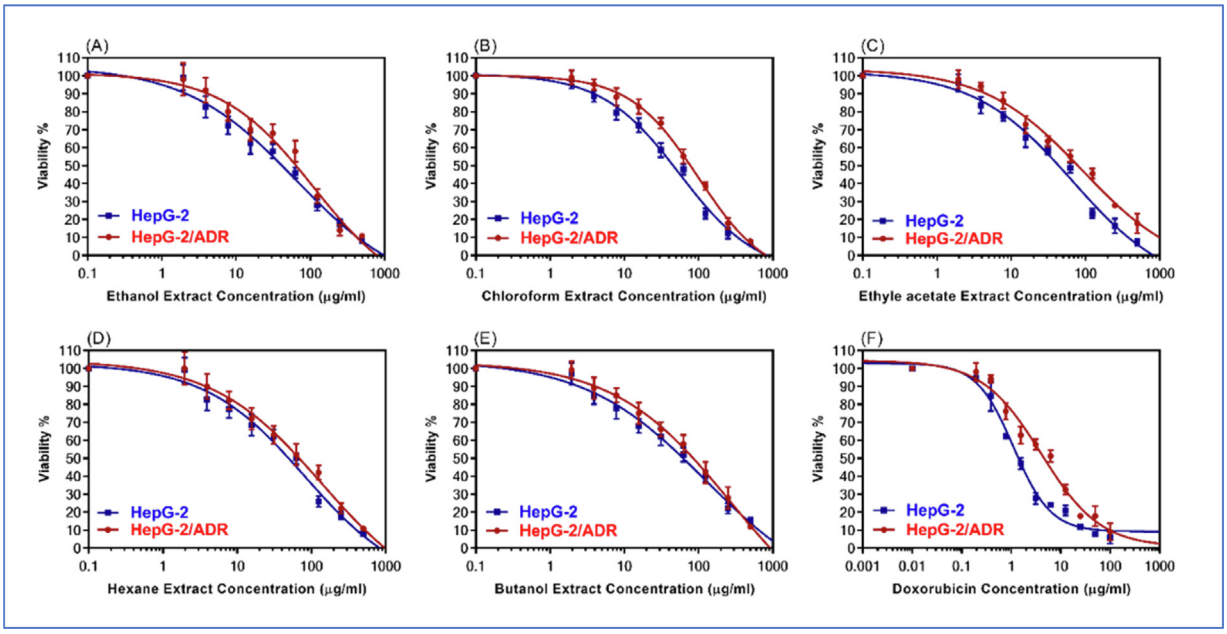

Fig. 3 The dose-response curves of *S. vermiculata* fractions A) ethanol, (B) chloroform, (C) ethyl acetate, (D) *n*-hexane, (E) *n*-butanol fractions, in comparison to (F) DOX in wild types HepG-2, and resistant-HepG-2/ADR cell lines.

Table 2 The IC_{50} values of the *S. vermiculata* extract/ fractions in comparison to DOX in HepG-2 wild types, and HepG-2/ADR resistant cell lines, with their relative resistance (RR) values using MTT assays.

***S. vermiculata* extract/ fractions**	**IC_{50} (µg/ml)**		**RR**
	HepG-2	**HepG-2/ADR**	
Ethanol	56.19 ± 4.41	100.5 ± 0.89	1.79
Chloroform	64.45 ± 5.57	110.1 ± 1.91	1.71
Ethyl acetate	66.68 ± 4.93	91.82 ± 0.72	1.38
n-Hexane	81.51 ± 6.91	138.2 ± 1.29	1.70
n-Butanol	125 ± 7.99	265.7 ± 0.14	2.13
Doxorubicin (DOX)	1.3 ± 0.11	4.77 ± 1.81	3.67

mechanism of drug protein interactions, the compounds identified in different sub-extracts of the partitioned alcoholic extract were subjected to molecular docking studies using Autodock vina® software program. A literature search showed that ABC transporter inhibitors binds to the substrate binding domains, or to the ATP-binding domains. Therefore, the molecular dockings were performed to explore the binding potentials in the substrate binding domains, as well as ATP-binding domains. The crystal structures used to explore the substrate binding region were 6FN1, 6FFC, and 5UJA representing ABCB1, ABCC1, and ABCG2 class of efflux proteins, respectively. The binding potential in the nucleotide, or ATP-binding domain were explored using 2CBZ. Before performing the molecular docking for the identified compounds, grid size were optimized by reproducing the binding modes of co-crystalized ligands. The docking scores, or potential binding affinity (represented in kcal/mol) of the identified compounds, and DOX were compared with the binding affinity of the co-crystalized ligand (Table 4). In addition to the molecular dockings of the identified compounds, standard chemotherapeutic agent DOX was also docked into the substrate binding sites of the 6FN1, 6FFC, and 5UJA receptors. The docking scores of the DOX were −8.4, −10, and −9 kcal/mol, respectively, and these were noted to be marginally more than the docking scores of the co-crystalized ligands, thereby indicating good binding of the DOX at the substrate binding site of the transporter protein. In general, the docking scores for the co-crystallized ligand was found to be −9.5, −9.3 and −8.1 kcal/-mol, respectively, for the three proteins. Among the compounds identified from the fractionated alcoholic extract, the compounds **3**, **4**, **6**, **8**–**25**, **27,** and **32** (Table 1) showed good binding potentials. The potential binding affinity varied from the ∼ 7.5 to ∼ 11 kcal/mol for the docked ligands. The highest binding potential was observed for the compound **15** (isorhoifolin). The calculated binding affinity using Autodock vina® were noted to be −9.1, −11.1, and −11.0 kcal/mol for 6FN1, 6FFC, and 5UJA proteins, respectively. Similarly, the compound **8** (spiraeoside), **11** (quercetin-3,7-dirhamnoside), **12** (quercetin-3-glucoside-7-rhamnoside), **14** (luteolin-7-O-glucoside), **24** (apigenin-7-O-glucoside), showed the docking score of ∼ -10 kcal/mol in all the proteins used for the docking studies. For the ligands, compound **3** (chlorogenic acid), **9** (3-glu-3,4′,7-trihydorxy isoflavanone), **10** (kaempferol-3-neohe speridoside-7-rhamnoside), **13** (hyperoside), **16** (kaempferol-3 -neohesperidoside), **19** (vitexin), 21 (5-O-methyl visamminol), **22** (N-*trans*-feruloyltyramine), **23** (quercetin), **25** (rhamnetin), **32** (ginsenoside-Rh2), the predicted binding affinities were in the range of ∼−8 to −9 kcal/mol (Table 1, and Table 4).

In order to find the molecular level interactions, the amino acid (AA) residues in the 5 Å area of the co-crystalized ligands were analyzed (**Table S1**). It revealed that the substrate's binding site was mostly comprised of the hydrophobic AA residues. At the molecular level interactions, the ligands which showed

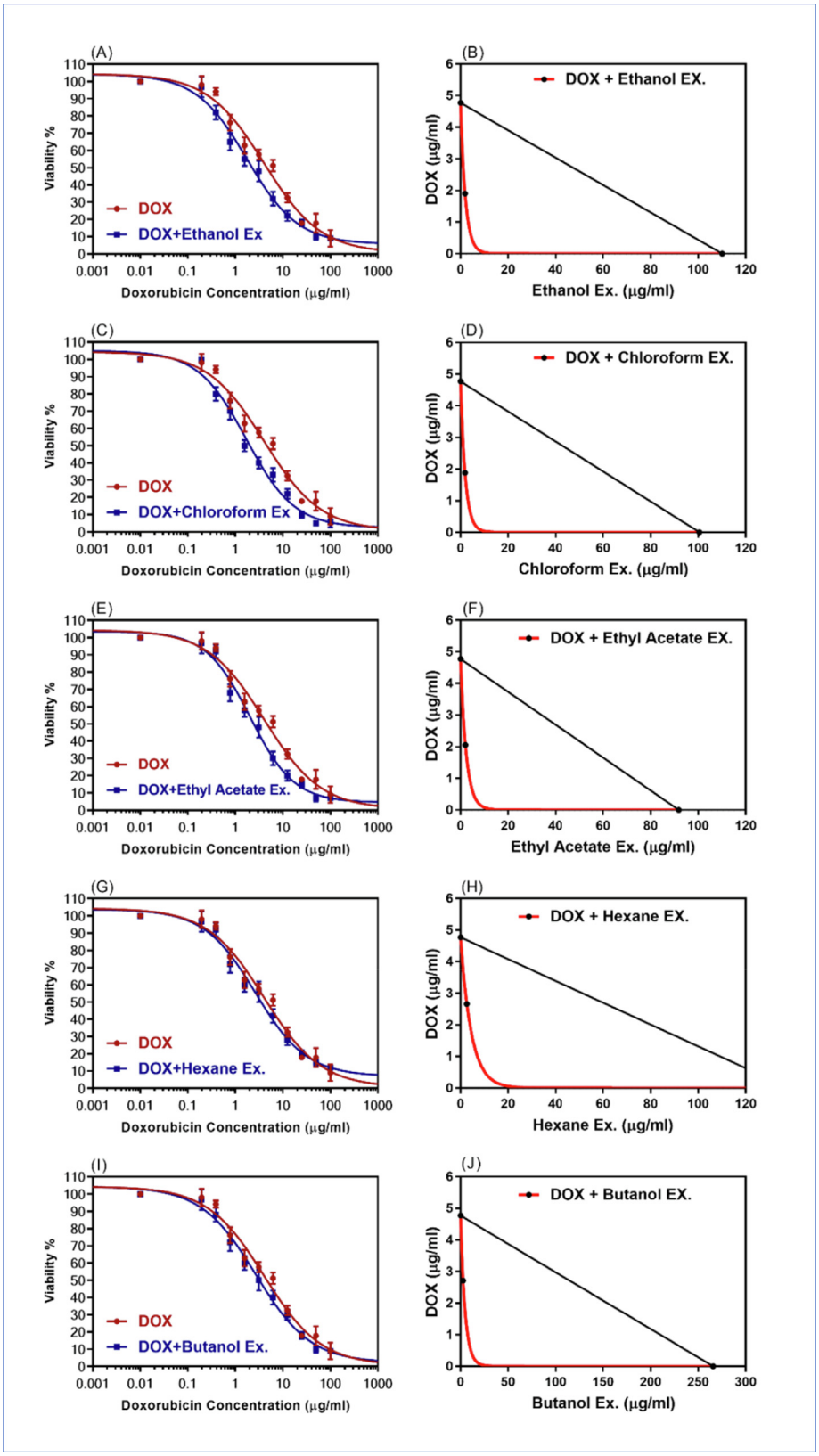

Fig. 4 The dose-response curves, and isobologram analysis of the combination of DOX with 20 µg/ml of *S. vermiculata* fractions (A-B) ethanol, (C-D) chloroform, (E-F) ethyl acetate, (G-H) *n*-hexane, (I-J) *n*-butanol in resistant HepG-2/ADR. The isobologram on the right side of the Figure showed the synergistic interactions between the DOX and the extract/fractions.

Table 3 Synergistic interactions of a combination of DOX with 20 μg/ml of *S. vermiculata* extract/fractions in resistant HepG-2/ADR cell lines, CI; combination index, FR; fold reversal, IB; isobologram, and medium effect equation (r-value).

***S. vermiculata* extract /fractions**	**IC_{50} (μg/ml)**	**Synergistic parameters**			
	HepG-2/ADR	**FR**	**CI**	**r**	**IB**
Doxorubicin (Dox)	4.77 ± 1.81	–	–	–	–
DOX + Ethanol Ex.	1.72^{***} ± 0.12	2.77	0.56	0.99	synergism
DOX + Chloroform Ex.	1.77^{***} ± 0.11	2.69	0.55	0.98	synergism
DOX + Ethyl acetate Ex.	2.05^{***} ± 0.19	2.33	0.65	0.99	synergism
DOX + *n*-Hexane Ex.	2.66^{**} ± 0.21	1.79	0.70	0.97	synergism
DOX + *n*-Butanol Ex.	2.71 ± 0.20	1.76	0.64	0.98	synergism

Table 4 Docking scores of different ligands and compounds docked in the substrate binding sites of 5UJA, 6FN1, and 6FFC proteins.*

Sr. No.	**Ligand/Compounds**	**5UJA**	**6FN1**	**6FFC**
1	Co-Crystalized ligand	−8.1	−9.5	−9.3
2	Doxorubicin	−9	−8.4	−10
3	3	−8.9	−8.6	−8.6
4	4	−8.6	−7.8	−9.6
5	6	−8.6	−8.2	−8.9
6	8	−10.6	−9.1	−10.7
7	9	−8.5	−7.9	−9.6
8	10	−8.8	−9.2	−9
9	11	−9.9	−9.6	−10.8
10	12	−10.2	−10	−9.4
11	13	−8.5	−8	−8
12	14	−10.8	−8.9	−10.8
13	15	−10.9	−9	−11.1
14	16	−9.3	−8.9	−9.1
15	17	−9.2	−8.5	−8.3
16	18	−8.7	−8.9	−9.9
17	19	−8.5	−9.1	−10.2
18	20	−10	−8.9	−9.4
19	21	−8.5	−7.3	−7.9
20	22	−8	−8.2	−9.2
21	23	−8.4	−8	−9.5
22	24	−10.5	−9.4	−10.4
23	25	−8.6	−7.6	−9.2
24	32	−9.2	−9.3	−8.8

* The docking score unit was kcal/mol; greater the negative scores, greater was the binding affinity.

the predicted binding affinity in the range of ∼−8.00 kcal/mol to −11 kcal/mol were considered. The major residues involved in hydrogen bondings in 1FN1 with the docked ligands were Asn^{295}, Asn^{720}, Gln^{724}, Gln^{772}, and Gln^{837}. Additionally, the AA residues, Gln^{989}, Gln^{841}, and Tyr^{306} were also found to be involved with few docked ligands. Similarly, for 5UJA, the commonly involved AA residues in hydrogen bonding were Trp^{553}, Asn^{590}, Arg^{593}, Asn^{984}, Tyr^{1235}, Gln^{1238}, Tyr^{1242}, and Asn^{1244}. Some of the AA involved with few other ligands were Gln^{1025}, Tyr^{1032}, and Asn^{1099}. For 6FFC, the AA involved in hydrogen bondings were Thr^{435}, Phe^{432}, Asn^{436}, and Phe^{439}. In addition to the later AA residues, Gln^{398} was also involved in hydrogen bonding with some of the docked ligands. It is also pertinent to mention that docking studies showed extensive hydrogen bondings for the docked ligands in protein crystal structure 5UJA, while limited hydrogen bonds were observed in the crystal structure of 6FFC, as compared to the 6FN1. The molecular docking studies, also displayed that the glycone part of the ligands were involved in extensive hydrogen bondings. Further, the hydrophobic interactions, such as, π – π stacking, and π – alkyl and aryl groups interactions were also noted in certain cases. These results showed that the majority of the compounds identified in the fractionated alcoholic extract of the *S. vermiculata* plant possess high binding affinity against ABC transporter family proteins, and therefore these products can be considered to be the likely MDR proteins inhibitors, and seemed to be involved in improving the sensitivity of the DOX in the HCC. The Fig. 4 showed the binding modes of isorhoifolin at the substrate binding site of ABCB1 (5UJA, **A**), ABCC1 (6FN1, **B**) and ABCG2 (6FFC, **C**). As mentioned above, the ATP-binding was also explored using molecular dockings. However, the results from the ATP-binding domain were not satisfactory to explain the experimental observations, and hence are not detailed out. The Fig. 5 represented the binding modes of compound **15** in the substrate binding site of the three proteins.

4. Discussion

The alcoholic extract of the *S. vermiculata* was sequentially partitioned using solvents of different polarities, starting from *n*-hexane, followed by ethyl acetate, chloroform, and *n*-butanol. The sequentially partitioned different fractions of the alcoholic extract was subjected to the LC-MS based chemical profilings, resulting in identifications of thirty six compounds from the different sub-extracts of the partitioned alcoholic extract. The substantial quantities of compounds identified from the sub-extracts were octadecanoic acid, palmitic acid, elaidic acid, kaempferol, ginsenoside-Rh2, linoleic acid, and 5,8,12-trihydroxy-9-octadecenoic acid. In addition, 6-gingerol, N-*trans*-feruloyltyramine, and quercetin-3-gluco side-7-rhamnoside, were also found in noticeable proportions. The LC-MS profiling also demonstrated the presence of compounds from different chemical classes that included phenolics, flavonoids, and expectedly fatty acids, as part of lipophilic constituents.

Different sub-extracts obtained from alcoholic extract were tested for their anti-HCC bioactivity using sensitive hepatic cell lines, and DOX-resistant HCC cell lines. As observed from the IC_{50} values of the DOX against the sensitive, and resistant-HCCcell lines, and in the absence as well as in presence of different sub-extracts of the partitioned fractions of the alcoholic extract, the synergism on the growth rate of resistant cancer cells was clearly visible, and this was further evident from

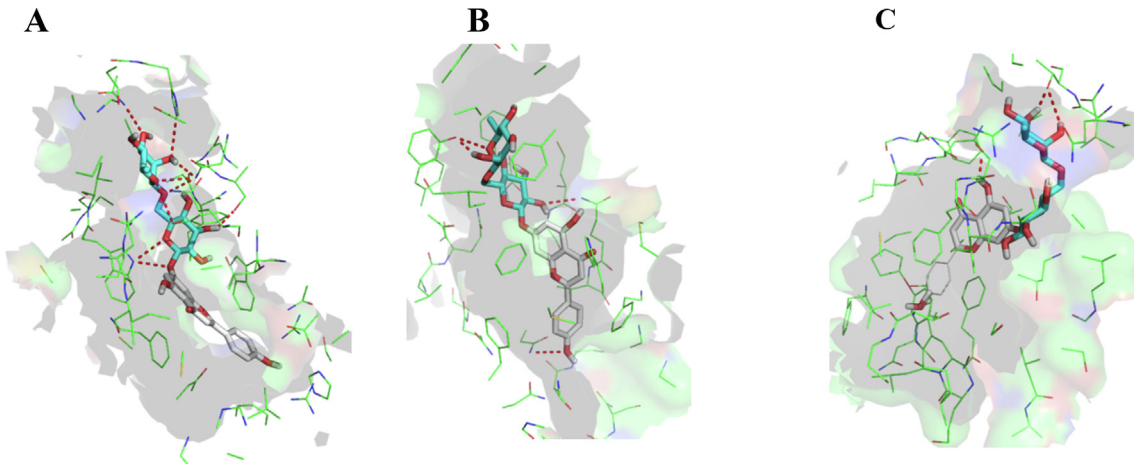

Fig. 5 The docked poses of the compound **15** in the substrate binding sites of ABCB1 (5UJA, **A**), ABCC1 (6FN1, **B**), and ABCG2 (6FFC, **C**).

the combination index listed in Table 3. The DOX is known to display less cellular inhibitions against the resistant cancer cells, as compared to the sensitive cancer cells, because of its efflux mediated through the ABC transporter family of proteins, or MDR-associated proteins. The synergism of DOX in combination with different sub-extracts may be attributed to modulation and/or competition for the substrate's binding site at the ABC-transporter family proteins. This finally resulted in reduction of DOX-efflux, and thereby enhanced its cellular accumulations. This hypothesis also gained strength from the fact that several compounds identified in different sub-extracts were flavonoids, which were explored for their inhibitory potential against the ABC transport proteins, which was evident from molecular docking studies. Good binding potentials of the flavonoids towards three classes of MDR-associated proteins, employed in this study, were in accordance with some of the earlier reported studies (Li and Paxton, 2013; Mohana et al., 2016)(Morris and Zhang, 2006). One of the known flavonoids which have been reported as MDR-associated protein modulator are quercetin and its glyosidic derivatives (Borska et al., 2010; Chen et al., 2010, 2018; Li et al., 2018; Mohana et al., 2016; Yuan et al., 2015), that were identified in the sub-extracts of the plant. Therefore, it can be safely envisioned that quercetin, and its structurally-related compounds are primarily responsible for the sensitization of the DOX-resistant HCC cells. In addition to the flavonoids, chlorogenic acid from *Coffee arabica* is also reported to exhibit modulating effects for the ABCB1 (P-gp) proteins (Wink et al., 2012), (Jang et al., 2008). Also, it is very well established that the ABC transporters are involved in wide-variety of substrates across the cell membranes, and therefore, it is possible that vitamin B2 acts as substrate, and competes with DOX for substrate binding site of the transporter proteins. The compounds **21**, **22**, and **32** also showed impressive binding potentials in the molecular modeling studies involving the three transporter proteins, however, a literature search using Scifinder® and Google® search engines revealed no evidence.

5. Conclusions

The alcoholic extract from *S. vermiculata* was subjected to sequential partitioning using *n*-hexane, ethyl acetate, chloroform, and *n*-butanol solvents, followed by LC-MS based chemical profiling of the obtained sub-extracts. The LC-MS profiling resulted in identification of thirty six compounds. Out of these, sixteen were flavonoids. The sub-extracts were tested for their anti-HCC activity against sensitive as well as doxorubicin (DOX)-resistant cell lines. The results displayed reversal of DOX-sensitivity in resistant-HCC cell lines. The reversal was found to be 2.7x, 2.33x, 1.79x, and 1.76x folds up in the chloroform, ethyl acetate, *n*-hexane and *n*-butanol sub-extracts, respectively. The molecular modelling of all thirty six identified compound against three ABC transporter family, i.e. ABCB1 (the MDR protein), ABCC1 (MRP protein), and ABCG2 (BCRP protein) displayed significant binding potentials of the flavonoids. Thus, presence of significant proportions of flavonoid compounds in these sub-extracts, in addition to the presence of chlorogenic acid, can be considered for the observed chemosensitizaton of the DOX-resistant HCC cell lines. The summative effects of the anti-hepatocellular cancer activity of the *S. vermiculta* extracts as experimentally observed in cell lines, were found to be interlinked owing to their constituents.

Declaration of Competing Interest

The authors declare that they have no known competing financial interests or personal relationships that could have appeared to influence the work reported in this paper.

Acknowledgements

The authors extend their appreciation to the Deputyship for Research & Innovation, Ministry of Education and, Saudi Arabia for funding this research work through the project number (QU-IF-1-2-2). The authors also thank the technical support of Qassim University.

Fundings

The authors extend their appreciation to the Deputyship for Research & Innovation, Ministry of Education and, Saudi Arabia for funding this research work through the project

number (QU-IF-1-2-2). The authors also thank the technical support of Qassim University.

Appendix A. Supplementary material

Supplementary data to this article can be found online at https://doi.org/10.1016/j.arabjc.2022.103950.

References

Alam, A., Kowal, J., Broude, E., Roninson, I., Locher, K.P., 2019. Structural insight into substrate and inhibitor discrimination by human P-glycoprotein. Science (80-.) 363, 753–756.

Al-Omar, M.S., Sajid, M.S.M., Alnasyan, N.S., Almansour, B.S., Alruthaya, R.M., Khan, R.A., Mohammed, S.A.A., Al-Damigh, A.M., Mohammed, H.A., 2021. The halophytic plant, Suaeda vermiculata Forssk extracts reduce the inflamed paw edema and exert potential antimicrobial activity. Pak. J. Bot 53, 1.

Al-Tohamy, R., Ali, S.S., Saad-Allah, K., Fareed, M., Ali, A., El-Badry, A., El-Zawawy, N.A., Wu, J., Sun, J., Mao, G.-H., 2018. Phytochemical analysis and assessment of antioxidant and antimicrobial activities of some medicinal plant species from Egyptian flora. J. Appl. Biomed. 16, 289–300.

Borska, S., Sopel, M., Chmielewska, M., Zabel, M., Dziegiel, P., 2010. Quercetin as a potential modulator of P-glycoprotein expression and function in cells of human pancreatic carcinoma line resistant to daunorubicin. Molecules 15, 857–870. https://doi.org/10.3390/molecules15020857.

Buchner, N., Krumbein, A., Rohn, S., Kroh, L.W., 2006. Effect of thermal processing on the flavonols rutin and quercetin. Rapid Commun. Mass Spectrom. An Int. J. Devoted to Rapid Dissem. Up-to-the-Minute Res. Mass Spectrom. 20, 3229–3235.

Bugde, P., Biswas, R., Merien, F., Lu, J., Liu, D.X., Chen, M., Zhou, S., Li, Y., 2017. The therapeutic potential of targeting ABC transporters to combat multi-drug resistance. Expert Opin. Ther. Targets 21, 511–530. https://doi.org/10.1080/14728222.2017.1310841.

Chen, Z., Huang, C., Ma, T., Jiang, L., Tang, L., Shi, T., Zhang, S., Zhang, L., Zhu, P., Li, J., Shen, A., 2018. Reversal effect of quercetin on multidrug resistance via FZD7/β-catenin pathway in hepatocellular carcinoma cells. Phytomedicine 43, 37–45. https://doi.org/10.1016/j.phymed.2018.03.040.

Chen, C., Zhou, J., Ji, C., 2010. Quercetin: a potential drug to reverse multidrug resistance. Life Sci. 87, 333–338. https://doi.org/10.1016/j.lfs.2010.07.004.

Choi, H.S., Cho, S.G., Kim, M.K., Kim, M.S., Moon, S.H., Kim, I.H., Ko, S.G., 2016. Decursin in Angelica gigas Nakai (AGN) Enhances Doxorubicin Chemosensitivity in NCI/ADR-RES Ovarian Cancer Cells via Inhibition of P-glycoprotein Expression. Phyther. Res. 30, 2020–2026. https://doi.org/10.1002/ptr.5708.

Cox, J., Weinman, S., 2016. Mechanisms of doxorubicin resistance in hepatocellular carcinoma. Hepatic Oncol. 3, 57–59.

Dallakyan, S., Olson, A.J., 2015. Small-molecule library screening by docking with PyRx. Chem. Biol., 243–250

Dohse, M., Scharenberg, C., Shukla, S., Robey, R.W., Volkmann, T., Deeken, J.F., Brendel, C., Ambudkar, S.V., Neubauer, A., Bates, S.E., 2010. Comparison of ATP-binding cassette transporter interactions with the tyrosine kinase inhibitors imatinib, nilotinib, and dasatinib. Drug Metab. Dispos. 38, 1371–1380. https://doi.org/10.1124/dmd.109.031302.

El-Awady, R., Saleh, E., Hashim, A., Soliman, N., Dallah, A., Elrasheed, A., Elakraa, G., 2017. The role of eukaryotic and prokaryotic ABC transporter family in failure of chemotherapy. Front. Pharmacol. 7, 1–15. https://doi.org/10.3389/fphar.2016.00535.

Frión-Herrera, Y., Gabbia, D., Díaz-García, A., Cuesta-Rubio, O., Carrara, M., 2019. Chemosensitizing activity of Cuban propolis and nemorosone in doxorubicin resistant human colon carcinoma cells. Fitoterapia 136,. https://doi.org/10.1016/j.fitote.2019.104173 104173.

Jang, M.H., Piao, X.L., Kim, J.M., Kwon, S.W., Park, J.H., 2008. Inhibition of cholinesterase and amyloid-&bgr; aggregation by resveratrol oligomers from Vitis amurensis. Phyther. Res. 22, 544–549. https://doi.org/10.1002/ptr.

Kalinowsky, L., Weber, J., Balasupramaniam, S., Baumann, K., Proschak, E., 2018. A diverse benchmark based on 3D matched molecular pairs for validating scoring functions. ACS Omega 3, 5704–5714.

Kim, S., Chen, J., Cheng, T., Gindulyte, A., He, J., He, S., Li, Q., Shoemaker, B.A., Thiessen, P.A., Yu, B., 2019. PubChem 2019 update: improved access to chemical data. Nucleic Acids Res. 47, D1102–D1109.

Kim, T.H., Shin, Y.J., Won, A.J., Lee, B.M., Choi, W.S., Jung, J.H., Chung, H.Y., Kim, H.S., 2014. Resveratrol enhances chemosensitivity of doxorubicin in multidrug-resistant human breast cancer cells via increased cellular influx of doxorubicin. Biochim. Biophys. Acta - Gen. Subj. 1840, 615–625. https://doi.org/10.1016/j.bbagen.2013.10.023.

Kumar, A., Jaitak, V., 2019. Natural products as multidrug resistance modulators in cancer. Eur. J. Med. Chem. 176, 268–291. https://doi.org/10.1016/j.ejmech.2019.05.027.

Le Grazie, M., Biagini, M.R., Tarocchi, M., Polvani, S., Galli, A., 2017. Chemotherapy for hepatocellular carcinoma: The present and the future. World J. Hepatol. 9, 907.

Lee, W.Y.W., Cheung, C.C.M., Liu, K.W.K., Fung, K.P., Wong, J., Lai, P.B.S., Yeung, J.H.K., 2010. Cytotoxic effects of tanshinones from Salvia miltiorrhiza on doxorubicin-resistant human liver cancer cells. J. Nat. Prod. 73, 854–859. https://doi.org/10.1021/np900792p.

Li, Y., Martin, R.C.G., 2011. Herbal medicine and hepatocellular carcinoma: applications and challenges. Evidence-Based Complement. Altern. Med. 2011.

Li, Z.-H., Guo, H., Xu, W.-B., Ge, J., Li, X., Alimu, M., He, D.-J., 2016. Rapid identification of flavonoid constituents directly from PTP1B inhibitive extract of raspberry (Rubus idaeus L.) leaves by HPLC–ESI–QTOF–MS-MS. J. Chromatogr. Sci. 54, 805–810.

Li, K., Lai, H., 2017. TanshinoneIIA enhances the chemosensitivity of breast cancer cells to doxorubicin through down-regulating the expression of MDR-related ABC transporters. Biomed. Pharmacother. 96, 371–377. https://doi.org/10.1016/j.biopha.2017.10.016.

Li, Y., Paxton, J.W., 2013. The effects of flavonoids on the ABC transporters: consequences for the pharmacokinetics of substrate drugs. Expert Opin. Drug Metab. Toxicol. 9, 267–285.

Li, S., Yuan, S., Zhao, Q., Wang, B., Wang, X., Li, K., 2018. Quercetin enhances chemotherapeutic effect of doxorubicin against human breast cancer cells while reducing toxic side effects of it. Biomed. Pharmacother. 100, 441–447. https://doi.org/10.1016/j.biopha.2018.02.055.

Longley, D.B., Johnston, P.G., 2005. Molecular mechanisms of drug resistance. J. Pathol. 205, 275–292. https://doi.org/10.1002/path.1706.

March, R.E., Miao, X.-S., 2004. A fragmentation study of kaempferol using electrospray quadrupole time-of-flight mass spectrometry at high mass resolution. Int. J. Mass Spectrom. 231, 157–167.

Mohammed, H.A., 2020. Behavioral evaluation of the effects of aqueous and ethanol extracts of suaeda vermiculata forssk on rats. Cent. Nerv. Syst. Agents Med. Chem. (Formerly Curr. Med. Chem. Nerv. Syst. Agents) 20, 122–127.

Mohammed, H.A., Al-Omar, M.S., Aly, M.S.A., Hegazy, M.M., 2019a. Essential oil constituents and biological activities of the halophytic plants, Suaeda Vermiculata Forssk and Salsola Cyclophylla Bakera Growing in Saudi Arabia. J. Essent. Oil Bear. Plants, 1–12.

Mohammed, H.A., Al-Omar, M.S., El-Readi, M.Z., Alhowail, A.H., Aldubayan, M.A., Abdellatif, A.A.H., 2019b. Formulation of ethyl cellulose microparticles incorporated pheophytin A isolated from Suaeda vermiculata for antioxidant and cytotoxic activities. Molecules 24, 1501.

Mohammed, H.A., Al-Omar, M.S., Khan, R.A., Mohammed, S.A.A., Qureshi, K.A., Abbas, M.M., Al Rugaie, O., Abd-Elmoniem, E., Ahmad, A.M., Kandil, Y.I., 2021. Chemical profile, antioxidant, antimicrobial, and anticancer activities of the water-ethanol extract of pulicaria undulata growing in the oasis of central Saudi Arabian desert. Plants 10, 1811.

Mohammed, S.A.A., Khan, R.A., El-Readi, M.Z., Emwas, A.-H., Sioud, S., Poulson, B.G., Jaremko, M., Eldeeb, H.M., Al-Omar, M.S., Mohammed, H.A., 2020a. Suaeda vermiculata aqueous-ethanolic extract-based mitigation of ccl4-induced hepatotoxicity in rats, and hepg-2 and hepg-2/adr cell-lines-based cytotoxicity evaluations. Plants 9, 1291.

Mohammed, S.A., Khan, R.A., El-Readi, M.Z., Emwas, A.H., Sioud, S., Poulson, B.G., Jaremko, M., Eldeeb, H.M., Al-Omar, M.S., Mohammed, H.A., 2020b. Suaeda vermiculata aqueous-ethanolic extract-based mitigation of CCl4-induced hepatotoxicity in rats, and HepG-2 and HepG-2/ADR cell-lines-based cytotoxicity evaluations. Plants 9, 1291. https://doi.org/10.3390/plants9101291.

Mohana, S., Ganesan, M., Agilan, B., Karthikeyan, R., Srithar, G., Beaulah Mary, R., Ananthakrishnan, D., Velmurugan, D., Rajendra Prasad, N., Ambudkar, S.V., 2016. Screening dietary flavonoids for the reversal of P-glycoprotein-mediated multidrug resistance in cancer. Mol. Biosyst. 12, 2458–2470. https://doi.org/10.1039/c6mb00187d.

Morris, G.M., Huey, R., Lindstrom, W., Sanner, M.F., Belew, R.K., Goodsell, D.S., Olson, A.J., 2009. AutoDock4 and AutoDockTools4: automated docking with selective receptor flexibility. J. Comput. Chem. 30, 2785–2791.

Morris, M.E., Zhang, S., 2006. Flavonoid-drug interactions: effects of flavonoids on ABC transporters. Life Sci. 78, 2116–2130. https://doi.org/10.1016/j.lfs.2005.12.003.

Ng, I.O.L., Liu, C.L., Fan, S.T., Ng, M., 2000. Expression of P-glycoprotein in hepatocellular carcinoma: a determinant of chemotherapy response. Am. J. Clin. Pathol. 113, 355–363.

Nies, A.T., König, J., Pfannschmidt, M., Klar, E., Hofmann, W.J., Keppler, D., 2001. Expression of the multidrug resistance proteins MRP2 and MRP3 in human hepatocellular carcinoma. Int. J. Cancer 94, 492–499.

O'Boyle, N.M., Banck, M., James, C.A., Morley, C., Vandermeersch, T., Hutchison, G.R., 2011. Open babel: an open chemical toolbox. J. Cheminform. 3, 1–14.

Orlando, B.J., Liao, M., 2020. ABCG2 transports anticancer drugs via a closed-to-open switch. Nat. Commun. 11, 1–11. https://doi.org/10.1038/s41467-020-16155-2.

Shawky, A.M., Abdalla, A.N., Ibrahim, N.A., Abourehab, M.A. S., Gouda, A.M., 2021. Discovery of new pyrimidopyrrolizine/indolizine-based derivatives as P-glycoprotein inhibitors: Design, synthesis, cytotoxicity, and MDR reversal activities. Eur. J. Med. Chem. 218,. https://doi.org/10.1016/j.ejmech.2021.113403 113403.

Shen, D., Hu, W., Zhao, S., Mao, C., 2021. Rapid naked-eye detection of a liver disease biomarker by discovering its monoclonal antibody to functionalize engineered red-colored bacteria probes. ACS Omega 1–6. https://doi.org/10.1021/acsomega.1c04779.

Silverman, J.A., Thorgeirsson, S.S., 1995. Regulation and function of the multidrug resistance genes in liver. Prog. Liver Dis. 13, 101–123.

Szakács, G., Paterson, J.K., Ludwig, J.A., Booth-Genthe, C., Gottesman, M.M., 2006. Targeting multidrug resistance in cancer. Nat. Rev. Drug Discov. 5, 219–234. https://doi.org/10.1038/nrd1984.

Trott, O., Olson, A.J., 2010. AutoDock Vina: improving the speed and accuracy of docking with a new scoring function, efficient optimization, and multithreading. J. Comput. Chem. 31, 455–461.

Wang, X., Shao, X., Zhang, W., Sun, T., Ding, Y., Lin, Z., Li, Y., 2022. Genus Suaeda: advances in phytology, chemistry, pharmacology and clinical application (1895–2021). Pharmacol. Res. 106203.

Wang, C., Huang, L., Li, R., Wang, Y., Wu, X., Shang, D., 2021. Synergistic therapy of doxorubicin with cationic anticancer peptide L-K6 reverses multidrug resistance in MCF-7/ADR cancer cells in vitro via P-glycoprotein inhibition. Int. J. Pept. Res. Ther. 27, 2291–2301.

Wink, M., Ashour, M.L., El-Readi, M.Z., 2012. Secondary metabolites from plants inhibiting ABC transporters and reversing resistance of cancer cells and microbes to cytotoxic and antimicrobial agents. Front. Microbiol. 3, 1–15. https://doi.org/10.3389/fmicb.2012.00130.

Wu, C.P., Li, Y.Q., Hung, T.H., Chang, Y.T., Huang, Y.H., Wu, Y.S., 2021. Sophoraflavanone G resensitizes ABCG2-overexpressing multidrug-resistant non-small-cell lung cancer cells to chemotherapeutic drugs. J. Nat. Prod. 84, 2544–2553. https://doi.org/10.1021/acs.jnatprod.1c00584.

Xing, Y., Wang, Z.H., Ma, D.H., Han, Y., 2014. FTY720 enhances chemosensitivity of colon cancer cells to doxorubicin and etoposide via the modulation of P-glycoprotein and multidrug resistance protein 1. J. Dig. Dis. 15, 246–259. https://doi.org/10.1111/1751-2980.12131.

Yuan, Z., Wang, H., Hu, Z., Huang, Y., Yao, F., Sun, S., Wu, B., 2015. Quercetin inhibits proliferation and drug resistance in KB/VCR oral cancer cells and enhances its sensitivity to vincristine. Nutr. Cancer 67, 126–136. https://doi.org/10.1080/01635581.2015.965334.